International Journal of Pharmaceutics 646 (2023) 123420

Contents lists available at ScienceDirect

International Journal of Pharmaceutics

journal homepage: www.elsevier.com/locate/ijpharm

Evaluation of tumor growth remission in a murine model for subcutaneous solid tumors – Benefits of associating the antitumor agent crotamine with mesoporous nanosilica particles to achieve improved dosing frequency and efficacy

William Yoshio Oyadomari [a,b,1], Gabriel Lessa Anthero [a,1], Marcos R. de A. Silva [c], Lucas C. Porta [a], Vitor Oliveira [b], Paul F. Reid [d], Osvaldo A. Sant'Anna [e], Wendel A. Alves [c], João V. Nani [a], Mirian Akemi Furuie Hayashi [a,*]

[a] Laboratory of Molecular Pharmacology, Departamento de Farmacologia, Escola Paulista de Medicina (EPM), Universidade Federal de São Paulo (UNIFESP), Brazil
[b] Departamento de Biofísica, Escola Paulista de Medicina (EPM), Universidade Federal de São Paulo (UNIFESP), Brazil
[c] Centro de Ciências Naturais e Humanas, Universidade Federal do ABC (UFABC), Brazil
[d] Celtic Biotech, Ireland
[e] Laboratory of Immunochemistry, Instituto Butantan, São Paulo, Brazil

ARTICLE INFO

Keywords:
Crotamine
Antitumor activity
Melanoma B16F10 cells
Mesoporous SBA-15 silica

ABSTRACT

Crotamine is a highly cationic polypeptide first isolated from South American rattlesnake venom, which exhibits affinity for acidic lysosomal vesicles and proliferating cells. This cationic nature is pivotal for its *in vitro* cytotoxicity and *in vivo* anticancer actions. This study aimed to enhance the antitumor efficacy of crotamine by associating it with the mesoporous SBA-15 silica, known for its controlled release of various chemical agents, including large proteins. This association aimed to mitigate the toxic effects while amplifying the pharmacological potency of several compounds. Comprehensive characterization, including transmission electron microscopy (TEM), dynamic light scattering (DLS), and zeta potential analysis, confirmed the successful association of crotamine with the non-toxic SBA-15 nanoparticles. The TEM imaging revealed nanoparticles with a nearly spherical shape and variations in uniformity upon crotamine association. Furthermore, DLS showed a narrow unimodal size distribution, emphasizing the formation of small aggregates. Zeta potential measurements indicated a distinct shift from negative to positive values upon crotamine association, underscoring its effective adsorption onto SBA-15. Intraperitoneal or oral administration of crotamine:SBA-15 in a murine melanoma model suggested the potential to reduce the frequency of crotamine doses without compromising efficacy. Interestingly, while the oral route enhanced the antitumor efficacy of crotamine, pH-dependent release from SBA-15 was observed. Thus, associating crotamine with SBA-15 could reduce the overall required dose to inhibit solid tumor growth, bolstering the prospect of crotamine as a potent anticancer agent.

1. Introduction

Crotamine is a natural cell-penetrating peptide that was first isolated from a South American rattlesnake (*Crotalus durissus terrificus)* venom with various biological properties, such as antitumor and antimicrobial activities, suggesting its potential as a chemotherapeutic agent (Yamane et al., 2013; Hayashi et al., 2022; Porta et al., 2022). In addition, this polypeptide, rich in basic amino acid residues, shows a high specificity for actively proliferating cells with a concentration-dependent cytotoxic effect, which is dependent on the disruption of lysosomes and subsequent activation of intracellular proteases, including cathepsins and caspases (Nascimento et al., 2007; Porta et al., 2022). The loss of

* Corresponding author.
E-mail addresses: william.yoshio@unifesp.br (W.Y. Oyadomari), gabriel.lessa@unifesp.br (G.L. Anthero), marcos.araujo@ufabc.edu.br (M.R.A. Silva), lucas.porta@unifesp.br (L.C. Porta), vitor.oliveira@unifesp.br (V. Oliveira), paul.reid@celticbiotech.com (P.F. Reid), osvaldo.santanna@butantan.gov.br (O.A. Sant'Anna), mhayashi@unifesp.br (W.A. Alves), joao.nani@unifesp.br (J.V. Nani), mhayashi@unifesp.br (M.A.F. Hayashi).
[1] These authors contributed equally to this work.

https://doi.org/10.1016/j.ijpharm.2023.123420
Received 11 April 2023; Received in revised form 6 September 2023; Accepted 15 September 2023
Available online 29 September 2023

mitochondrial membrane potential, and rapid intracellular calcium release and intracellular calcium overload was also demonstrated to be involved in this cytotoxic property of crotamine (Nascimento et al., 2007; Nascimento et al., 2012). The well-known *in-vivo* toxic effect of crotamine is the reversible hind limb paralysis observed in rodents (but not in human), which was demonstrated by us to involve the action on voltage-gated ion channels present in skeletal muscles (Lima et al., 2018). We also demonstrated the tumor specific accumulation of crotamine, administered by the intraperitoneal (ip) route in mouse models bearing subcutaneous solid tumors, by employing a noninvasive optical imaging procedure that permitted real-time *in-vivo* monitoring of crotamine uptake by isolated solid tumor tissue formed by subcutaneous injection of murine melanoma B16F10 and/or mice mammary carcinoma TS/A-pc cells (Nascimento et al., 2012). Daily administration of crotamine by ip (1 μg/animal) or oral (10 μg/animal) routes for 21 consecutive days significantly reduced the tumor growth in mice bearing isolated implanted subcutaneous tumors, as well as increased animal survival rates (Pereira et al., 2011; Campeiro et al., 2018). More importantly, the doses of crotamine necessary for these pharmacological effects were far below of those reported to be needed to observe any hind limb paralysis or animal death (Lima et al., 2018). Additionally, crotamine administered orally to healthy mice was demonstrated to stimulate the differentiation/activation of brown adipocytes, leading to increased energy expenditure and stimulation of a pro-thermogenic phenotype, although this effect was not evident in mice bearing subcutaneous solid tumors (Marinovic et al., 2018). This observation confirmed the preferential tropism and accumulation of crotamine in tumor tissue, as demonstrated by *in-vivo* real-time monitoring (Nascimento et al., 2012). Recent advances of brown adipocyte tissue (BAT) function in the metabolic aspect have suggested a relationship between BAT and cancer cachexia, which is a pathological process accompanied with decreased body weight and increased energy expenditure in cancer patients (Dong et al., 2018). While the possible cancer cachexia effect of crotamine was ruled out in a previous work, crotamine revealed additional advantages, including the improved glucose tolerance and increased insulin sensitivity, accompanied by a reduction of plasma lipid levels and decreased levels of biomarkers of liver damage and kidney disfunctions. There was also a significant reduction in white adipose tissue (WAT) and increase in BAT mass observed in healthy mice not bearing tumors (Marinovic et al., 2018). The development of drugs capable of increasing the volume and/or activity of BAT could pave the way to translational strategies aiming to help control animal metabolism, potentially by reducing obesity and insulin resistance (Dong et al., 2018). Interestingly, oral administration of crotamine showed improved efficacy to increase the capacity of glucose clearance and insulin secretion in healthy animals, with significant increase in adipocyte browning and BAT size, probably by modulating voltage-gated K^+ channels and promoting Ca^{2+} release from intracellular stores (Campeiro et al., 2018; Marinovic et al., 2018). These important attributes of crotamine and this application is also being studied by us, and may also represent a crucial characteristic for this compound action as an antitumor agent, as it provides an extra therapeutic advantage that will be further explored by us in the near future, once the best dosing and treatment regimen condition for antitumor therapy is determined. However, the potential applications of crotamine could be also improved by a reduction in dose levels and by overcoming the need of daily administration regimen employed by us up to now.

Drug delivery systems have received increasing attention since early 2000s, motivated by the upmost priority to increase drug safety and efficacy. However, they can also be used to decrease the dosing frequency to help optimize any specific treatment regimen. Mesoporous silica was demonstrated to be biocompatible, with the advantage of a higher physiochemical and biochemical stability compared to other inorganic materials, as well as with high drug loading capacity, tunable pore size, pore volume, and high surface area. This material is thus suitable for many applications and an ideal option for controlled and targeted drug delivery by protecting small molecules from harsh environments (Schlossbauer et al., 2011; Yoo et al., 2011; Sant'Anna et al., 2019; Sant'Anna et al., 2020). Mesoporous silica shows a high density of silanol groups, which can link to diverse drug molecules allowing ordered mesoporous SBA-15 silica to be widely used for the controlled release of many different therapeutic compounds (Lopez et al., 2009; García-Muñoz et al., 2014; Tan et al., 2015; Rehman et al., 2016; Rehman et al., 2023). In fact, the ability of SBA-15 silica to reduce toxicity and potentiate the pharmacological activity of different compounds has also been widely demonstrated by many others (Cai et al., 2021; Dadej et al., 2022a; Dadej et al., 2022b; Predarska et al., 2022). Recently, it was also demonstrated that the main neurotoxin of *Crotalus durissus terrificus* venom, named crotoxin, whose potential toxicity remains as a limiting factor in its therapeutic use as an anti-inflammatory and antinociceptive compound, and its toxicity was reduced while its analgesic effect was enhanced by using this inert nanostructured mesoporous silica as a delivery vehicle (Sant'Anna et al., 2019; Sant'Anna et al., 2020).

The goal of the present work was to evaluate the effects and possible advantage of combining crotamine with ordered mesoporous SBA-15 silica to create a slow delivery system that avoids the concentration spikes in serum following administrations by bolus injection and, therefore, decrease the dose and frequency of drug administration.

2. Materials and methods

2.1. Reagents and cell lines

The ordered mesoporous SBA-15 silica was synthesized using poly [ethylene oxide]-poly[propylene oxide]-poly[ethylene oxide] triblock copolymer [Pluronic P123, $EO_{20}PO_{70}EO_{20}$, MW = 5800-BASF], tetraethyl orthosilicate [TEOS] (Fluka Analytical Sigma-Aldrich, Merck KGaA, Darmstadt, Germany), and hydrochloric acid (Thermo Fisher Scientific Inc., Hampton, NH, USA), as previously described (Matos et al., 2001). This silica was kindly provided by Dr. Osvaldo Sant'Anna (Instituto Butanan, SP, Brazil). The X-ray Diffraction (XRD) characterization was also performed as in a previous work (Fantini et al., 2004). Synthetic full-length crotamine was commercially purchased from Smartox Biotechnology (Saint-Egreve, France). The crotamine adsorption in the SBA-15 was performed by simple incubation in a water solution followed by dilution in saline or water (for intraperitoneal (ip) and oral route administration, respectively) aiming to achieve crotamine:SBA-15 (1:1) complex to permit the administration of volumes of 100 μL/kg for intraperitoneal route or 100 μL/animal for oral delivery), as reported elsewhere (Campeiro et al., 2018; Marinovic et al., 2018; Porta et al., 2022).

2.2. Dynamic light scattering (DLS) and zeta potential

DLS measurements were carried out using a platform-based ALV/CGS-3 goniometer system (ALV GmbH), furnished with a polarized HeNe laser (22 mW) that has a wavelength of 633 nm, a 7004 digital correlator, and a pair of crosswise operating pseudocorrelation detectors (APD). A glass cuvette (optical path: 5 mm) containing 1 mL of each sample (at the same concentration used for biological tests) was employed, except for isolated crotamine, as the peptide is too small to be analyzed by DLS. The temperature was maintained at 25 °C throughout the measurements, which were conducted in triplicate.

Zeta potential measurements were performed using a Malvern Zetasizer nano series, utilizing a disposable folded capillary cell containing 1 mL of each sample (at the same concentration used for biological tests). The Smoluchowski approximation was adopted, wherein Henry's equation considered a value of f(ka) = 1.5 to model the particle with spherical geometry in an aqueous solution (Zholkovskij et al., 2007).

For both experiments, an aqueous silica stock solution with a 1 mg/

mL concentration was prepared and allowed to stand for 24 h. After this period, 1 mL of the supernatant was collected and centrifuged for 10 min at 10,000 rpm. Samples for DLS and zeta potential experiments were prepared using the supernatant from this centrifuged solution. The sample containing only the silica nanoparticle (SBA-15) consisted of 100 μL of the stock mentioned above mixed with 900 μL of deionized water. The sample containing silicon nanoparticles functionalized with the crotamine peptide (CROT) comprised 100 μL of the silica stock solution, 50 μL of a 1 mg/mL crotamine peptide solution, and 850 μL of pure water.

2.3. Transmission electron microscopy (TEM)

High-resolution transmission electron microscopy (HRTEM) analyses were conducted using a Talos F200X G2 transmission electron microscope (Thermo Scientific) equipped with a field-emission gun (FEG-X) and a scanning transmission electron microscopy (STEM) module, operating at an acceleration voltage of 200 keV.

For image acquisition, 4 μL of each sample solution (SBA-15 and crotamine:SBA-15) were applied onto transmission substrates (holey carbon-coated grids constructed from type B carbon film supported on a 400 mesh copper grid) and allowed to dry for 24 h in a vacuum desiccator.

2.4. Crotamine release assay

In vitro drug release profiles were evaluated in simulated fluids, prepared by dissolving 8.06 g NaCl; 0.22 g KCl; 1.15 g Na_2HPO_4; 0.2 g KH_2PO_4 in 1 L of deionized water, pH 7.4; or 7.45 g KCl; 0.8 cm^3 HCl in 1 L of deionized water, pH 2.0. Each 10 μg of crotamine adsorbed in 20 μg of SBA-15 mesoporous nanosilica was placed in 3 mL of simulated fluid at pH 2 or 7, at room temperature. All the analyses were performed in triplicate, using a high-performance liquid chromatography (HPLC) (Shimadzu 10AVP) monitored at 215 and 280 nm.

2.5. Animals

Male C57BL/6 mice, 6 to 8-weeks old, were obtained from the Animal Facility of the Federal University of São Paulo Medical School (EPM/ UNIFESP). The animals were maintained under controlled temperature (20–22 °C), light/dark cycle every 12 h, and groups of 4 animals were kept in Plexiglas cages (41 × 34 × 16.5 cm) supplied with water and food *ad libitum*. The animals were maintained in accordance with the guidelines of the Committee on Care and Use of Laboratory Animal Resources, National Research Council, USA. This study was approved by the Ethic Committee for Animal Use (CEUA) of UNIFESP/ EPM (N° 9212250520), and the experiments with the animals were performed in accordance with FELASA guidelines.

2.6. Cell preparation

B16F10 (ATCC CRL-6475) murine melanoma cells from American-Type Culture Collection (ATCC, Manassas, VA, USA) were cultured in DMEM (Thermo Fisher Scientific Inc.), supplemented with 10% fetal bovine serum (LGC Biotechnology, São Paulo, Brazil), containing penicillin 50 units/mL and streptomycin 50 μg/mL (Thermo Fisher Scientific Inc.), at 37 °C in a humidified atmosphere, with 5% CO_2. Culture medium was replaced every 2 days, and the cells were maintained up to reach semi-confluence during the cell amplification process. The cells were quantified using a Neubauer chamber and trypan blue 0.2% (1:1).

2.7. Cell culture assays with crotamine

Cell viability was evaluated by a colorimetric assay based on the ability of viable cells to reduce a soluble yellow tetrazolium salt [3-(4,5-dimethylthiazol-2-yl) 2,5-diphenyl tetrazolium bromide] (MTT) to a blue formazan crystal by mitochondrial succinate dehydrogenase activity of viable cells. The MTT assay was performed using B16F10 cells (3×10^3 cells/well) were plated in a 96-well plate, and crotamine alone [10 μg] or associated with mesoporous SBA-15 nanosilica (crotamine: SBA-15) [10 μg crotamine:20 μg SBA-15] or the nanosilica alone [20 μg] diluted in cell culture medium were added and incubated for 24 h, at 37 °C, 5% CO_2. Then, MTT solution (0.5 mg/mL) was added and the plates were maintained at 37 °C incubator for 4 h. Following this incubation, absorbance was measured at 570 nm in the SpectraMax M5 spectrometer (Molecular Devices, San Jose, CA, USA). The OD_{570} value of the control (without treatment) was considered as 100% of cell viability.

2.8. Tumor implantation and in-vivo treatment with crotamine

The tumor implants and *in-vivo* treatments were performed essentially as previously described (Campeiro et al., 2018; Marinovic et al., 2018). Animals (N = 101) received a single injection of 1×10^5 B16F10 melanoma cells in 200 μL of PBS, subcutaneously on experimental day 1 and the animals were randomly divided into the following groups: 1) control group receiving vehicle (0.9% saline, daily); 2) treated daily with crotamine alone; 3) treated daily with crotamine:SBA-15; 4) treated with crotamine:SBA-15 every 5 days; 5) treated with crotamine: SBA-15 every 10 days, keeping the doses of 1 μg of crotamine/animal by ip administration of crotamine alone or adsorbed in SBA-15 (2 μg/animal); in addition to 6) treated daily with crotamine alone; 7) treated daily with crotamine:SBA-15; 8) treated with crotamine:SBA-15 for every 5 days, in which groups 6–8 being by oral administration and with a dose of 10 μg of crotamine/animal of crotamine alone or adsorbed in SBA-15 (20 μg/animal). All treatment was accomplished by ip injection with 100 μL/animal or 200 μL/animal for oral route administration (oral gavage). The body weight of each animal was determined at the beginning of experiments, *i.e.* before treatment with crotamine, and every 3 days until the end of the experiment which lasted for 21 consecutive days for all groups. The treatment started on the same day of tumor cell injection. The sample size for each group in this study varied in accordance with the Guidelines for Tumor Induction in Rodents, which recognizes that animals with tumors that have a volume greater than the maximum allowed tumor volume, *i.e.* 2000 mm^3 for mice, should be excluded from the study. In addition, animals that exhibited tumor-related endpoints such as interference with eating, drinking, or ambulation were also excluded. For this reason, the control group with no treatment need to be usually larger to compensate the higher mortality usually observed in the groups with no treatment. As a result, a total of 101 animals were studied and they belonged to: Group 1: N = 26; Group 2: N = 13; Group 3: N = 10; Group 4: N = 17; Group 5: N = 13; Group 6: N = 7; Group 7: N = 8; Group 8: N = 7. The general health condition of the animals was also monitored at 3-days intervals along the 21-days treatment period. At the end of the experimentation period, the animals were then weighted for the last time and euthanized by decapitation. The tumor was then collected and weighted, as previously described (Campeiro et al., 2018; Marinovic et al., 2018; Porta et al., 2022), to evaluate the antitumor efficacy of ip or oral administration with crotamine and/or crotamine:SBA-15.

2.9. Statistical analysis

The normality of the data distributions was checked using the Shapiro-Wilk test, the homogeneity of variances was checked using Levene's test and sphericity was checked using Mauchly's test. Data analysis was performed using JAMOVI version 2.39 software. Depending on the distribution of variables, parametric tests such as Student's *t*-test and ANOVA were used. If the variables did not meet the homogeneity assumption, Welch's correction was applied, and if it did not meet the sphericity assumption, Greenhouse-Geiser correction was applied. The Z-score transformation method was used to detect outliers with a

threshold of ±2 standard deviations and when normality assumption did not suit. Graphs were generated using GraphPad Prism version 7.0 software (San Diego, CA, USA). A *p*-value of ≤0.05 was considered statistically significant for all statistical tests.

3. Results

3.1. Analysis of crotamine interaction with mesoporous SBA-15 silica using transmission electron microscopy (TEM), dynamic light scattering (DLS), and zeta potential measurements

TEM images indicate that both SBA-15 and SBA-15:crotamine nanoparticles have a nearly spherical shape. The average diameters are approximately 33.0 nm and 72.0 nm, respectively, and there is a significant decrease in the uniformity of silica particles, as shown in Fig. 1. This pattern suggests that peptide modifications might be taking place both at the interface and within the channel structure.

DLS curves for pure SBA-15 and SBA-15:crotamine (Fig. 2) depict a narrow unimodal size distribution. The average diameters are 224.7 ± 5.0 nm (PDI = 0.144) and 209.6 ± 2.60 nm (PDI = 0.095), respectively. This data suggests a propensity for both mesoporous silica nanoparticles to form minor aggregates. The Zeta potential for pure silica nanoparticles, due to the negatively charged silanol groups, is measured at −30.5 ± 3.25 mV. This value shifts positively to 8.39 ± 3.29 mV for SBA-15:crotamine. This shift from negative to positive zeta potential indicates the effective adsorption of crotamine onto the mesoporous SBA-15 silica, suggesting the presence of crotamine on the nanoparticle's external surface and a potential reduction in the density of free silanol groups.

3.2. Cytotoxic activity of crotamine associated with the mesoporous SBA-15 silica: Analysis by MTT assay

The cytotoxic effect of crotamine alone or associated with mesoporous SBA-15 silica was evaluated using mice melanoma B16F10 cells by MTT assay showing the adsorption by this nanosilica did not interfere in cytotoxicity of crotamine, while mesoporous nanosilica alone did not show cytotoxicity against this tumor cells (Fig. 3).

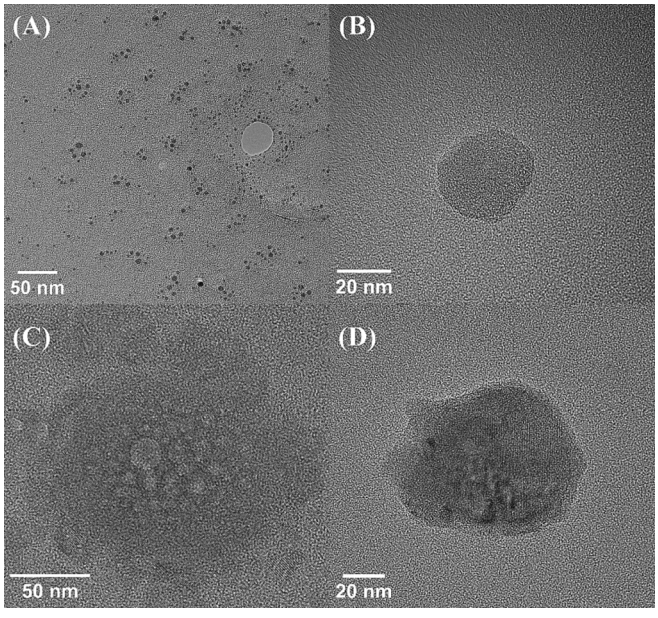

Fig. 1. Transmission Electron Microscopy (TEM) images of nanoparticles: SBA-15 in panels (A) and (B), and SBA-15@CRT in panels (C) and (D).

3.3. Drug release studies in pH 2.0 or 7.4

The influence of pH on crotamine release from SBA-15 mesoporous nanoparticle was carried out employing a buffer simulating the chemical environment in the stomach and peripheral fluids of a living mammalian organism. Our results show the strong influence of pH of the medium for the release process of crotamine (time, efficiency, etc.), with a significant faster release at more acidic (stomach) compared to neutral (parental fluids) conditions (Fig. 4), as also previously described for another toxin peptide from bees (Schlossbauer et al., 2011).

3.4. Treatment of the animals with crotamine alone or in combination with the ordered mesoporous SBA-15 silica by intraperitoneal (ip) or oral administration

The animals regularly gained weight during the experimental period, similarly in all evaluated groups, and with no significant difference ($F(4, 33) = 1.636$, $p = 0.189$) in the weight gain of the animals observed among the groups, during the treatment period. The main organs of the animals were also removed and weighted after euthanasia on the last day of treatment showing no significant difference in the main organs weight or in the length of the femur (as shown in Table 1), suggesting the absence of significant influence of these treatment protocols on general animal growth and development.

3.5. Tumor size

Evaluation of tumor growth inhibition following the daily treatment with crotamine alone, or with crotamine associated with the mesoporous SBA-15 silica (1:1), at a dose of 1 or 10 μg of crotamine/animal, through intraperitoneal (ip) or oral routes, respectively, revealed a significant reduction in tumor volume in animals relative to control animals receiving vehicle (saline or water, respectively) (F_{welch} (4, 74) = 6.55, $p = 0.0001$). Significant differences in tumor size were observed in animals treated orally with daily crotamine alone or combined with SBA-15 nanosilica (F_{welch} (3, 45) = 9.71, $p < 0.0001$), although no significant difference was found for the average tumor size with every 5 days treatment by oral route with crotamine combined with SBA-15 nanosilica compared with untreated control ($p = 0.9997$).

Interestingly, the treatment by intraperitoneal route with crotamine alone or crotamine:SBA-15 (1:1) complex, administered daily, every 5 days or every 10 days, showed a similar effect in tumor growth inhibition (Fig. 5). It is also worth emphasizing that the confidence interval (CI) is quite narrower for crotamine administration by oral route associated with SBA-15 (95% CI [0.1476, 1.050]) compared with the same treatment regimen with crotamine alone (95% CI [2.144, 4.073]), with a range of about 1,500 and 2,160, respectively. On the other hand, this range increased with the decreases of the administration frequency of the crotamine:SBA-15 for ip treatments, although the final mean size of tumor tissue was the same for all conditions of treatment with crotamine:SBA-15, namely daily, or every 5 or 10 days (range of 95% CI of mean of 2.771 (95% CI [0.6976, 1.010]), 3,675 (95% CI [0.932, 2.094]) or 3.682 (95% CI [1.006, 2.549]), respectively). These findings confirm the potential of crotamine as a standalone treatment or in combination with SBA-15 nanosilica for inducing tumor growth remission, supporting its further investigation as a potential therapeutic strategy in cancer treatment.

4. Discussion

Natural products have been considered as a rich source of compounds for the development of potential drugs for the treatment of several pathologies (Hayashi et al., 2012). Crotamine was previously demonstrated to inhibit tumor growth in an animal model of solid tumors induced by subcutaneous injection of B16F10 melanoma cells, following treatment with daily intraperitoneal (ip) or oral

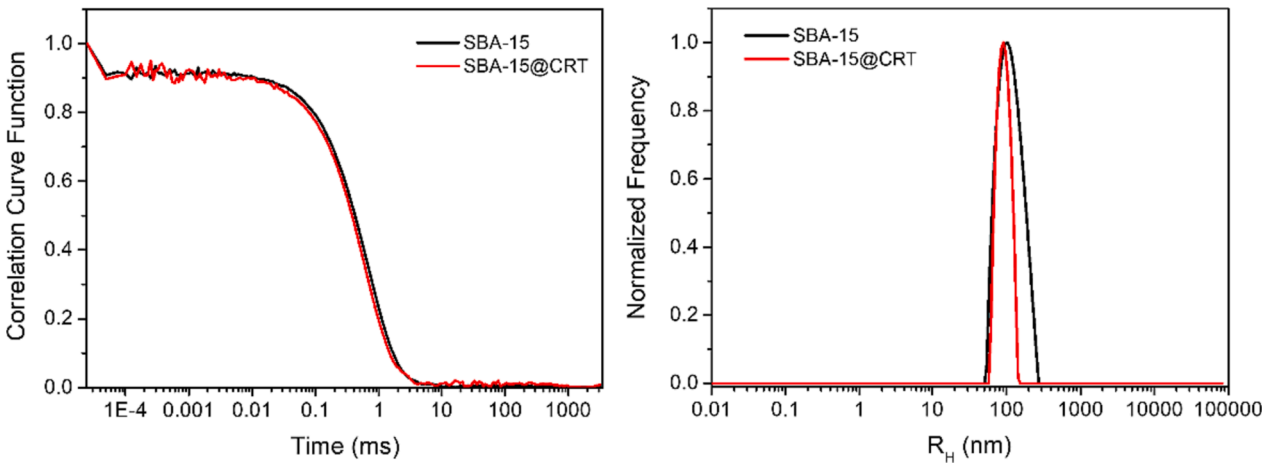

Fig. 2. DLS results for SBA-15 and SBA-15:crotamine (CRT). The left panel presents a correlation curve as a function of time, while the right panel depicts the normalized frequency versus hydrodynamic radius.

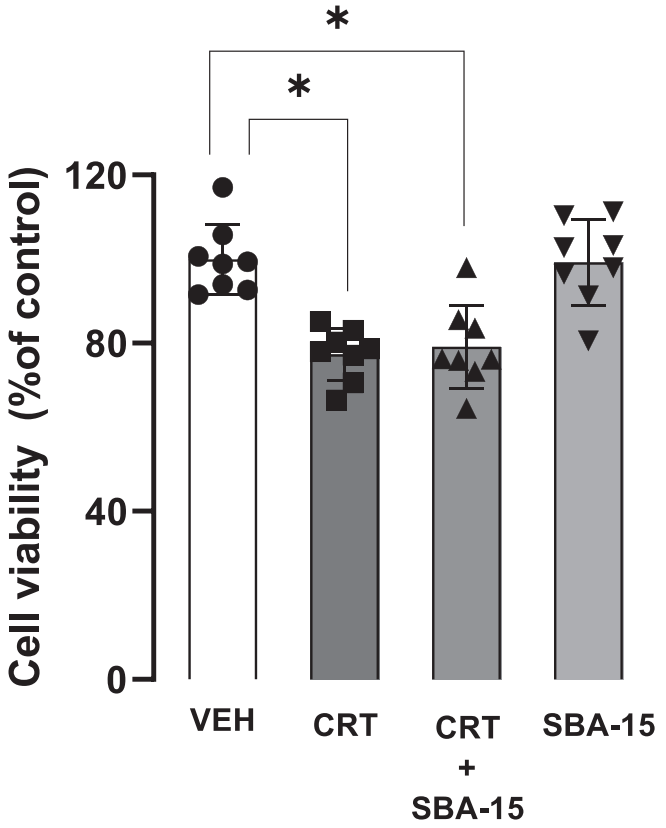

Fig. 3. Crotamine toxicity for cultured B16F10 cells. Cell viability assay of murine melanoma B16F10 cells treated with crotamine alone, associated with mesoporous SBA-15 nanosilica (crotamine:SBA-15) or nanosilica alone, for 24 h, was evaluated by MTT assay. The results correspond to a total of N = 8 for each evaluated condition, $*p \leq 0.05$ for one-way ANOVA test.

administration of crotamine alone for 21 days, and with no observable adverse effects (Pereira et al., 2011; Campeiro et al., 2018). The specific accumulation of crotamine in engrafted solid tumor tissues was also demonstrated by employing by employing a noninvasive optical imaging procedure that permitted real-time *in-vivo* monitoring of crotamine uptake by isolated solid tumor tissue formed by subcutaneous injection of murine melanoma B16F10 and/or mice mammary carcinoma TS/A-pc cells (Nascimento et al., 2012). Previously, we have also determined that the doses of crotamine needed to observe the *in vivo* toxicity (Lima et al., 2018) were far above those needed to guarantee a significant remission in tumor growth (Pereira et al., 2011; Campeiro et al., 2018). In addition, the cytotoxic effects of crotamine were also observed at very low doses, with an estimated IC_{50} value of about 1 μM (Hayashi et al., 2008). Concerns regarding the extraction of the peptide directly from venom related to the potential impacts to biodiversity and animal care, in addition to the risk of accidental contamination of the venom by adventitious agents that could be an unacceptable risk to patients, led us to characterize a chemically synthesized analog of full-length crotamine and confirm that this chemical analog had exactly the same features and properties of the native toxin. It may also allow further improvements in the pharmacological properties of this polypeptide by rational design (de Carvalho Porta et al., 2020). However, although allowing for production at large scale and under good manufacturing procedures (GMP), as would be required for preclinical and clinical assays to support the use of crotamine in human therapy, the cost of producing this peptide by chemical synthesis is still very high.

Therefore, aiming to decrease the amount of crotamine needed to continue preclinical studies and increase the chance of translating this potential therapeutic alternative to clinical setting, we have evaluated herein the combination of crotamine with ordered mesoporous SBA-15 silica, which was previously demonstrated by others to be an interesting vehicle to promote controlled release of the associated active compound. Although the mechanisms by which SBA-15 decreases the toxicity of compounds is still not clear, studies have shown that the SBA-15 surface allows high drug-loading with a controlled release of different compounds, which may be the basis for reduced toxicity of these drugs (Lu and Liong, 2011; Sant'Anna et al., 2019; Vieira et al., 2019; Cai et al., 2021; Dadej et al., 2022a; Dadej et al., 2022b; Predarska et al., 2022).

The adsorption of crotamine in mesoporous SBA-15 nanosilica was demonstrated here by XRD analysis, DLS and TEM images. The present study confirmed the advantages of associating crotamine as an antitumor agent with SBA-15 silica as it was possible to observe an effective antitumor activity, which was similar to that observed for daily treatment with crotamine alone, even after decreasing the crotamine administration frequency (from daily to every 5 or 10 days), with a concurrent decrease in total doses and/or amount of crotamine needed to inhibit tumor growth, particularly when employing the oral route. The association with this mesoporous nanosilica particles may also potentially contribute to reduce the risk of *in vivo* toxic effects, associated with concentration spikes in specific tissues of the animal. Under the conditions employed herein, the inhibition of tumor growth with 5- or 10-days treatment regimens was similar to that observed for daily treatments by ip route, while the treatment by oral route in 5-days

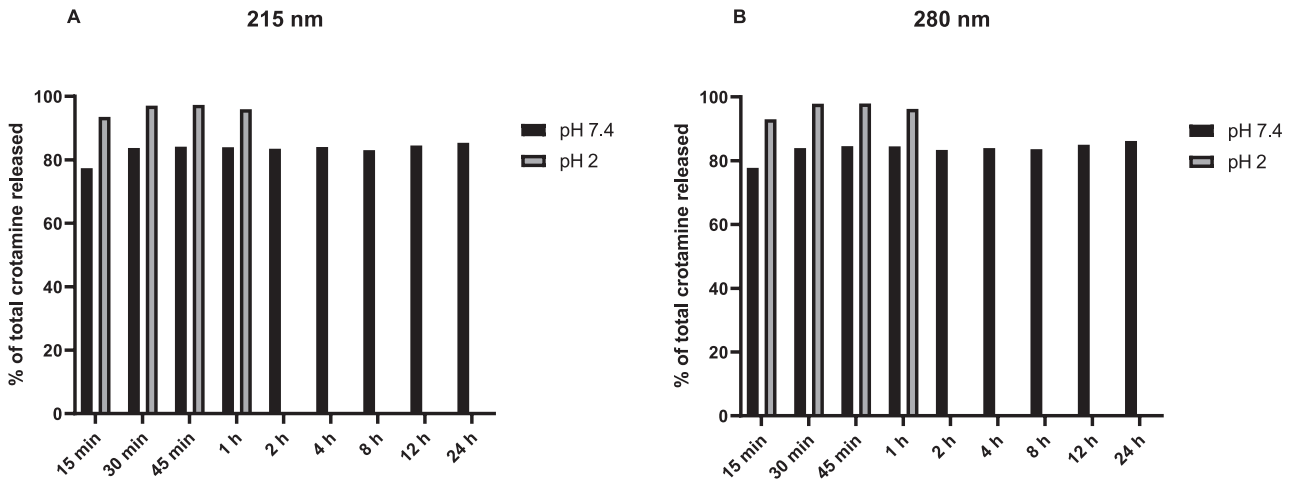

Fig. 4. Crotamine release over time, as measured by HPLC at 215 and 280 nm.

Table 1
Weight of the main organs and length of the femur of the animals.

	CONTROL (vehicle)	Injection route	CROTAMINE	CROTAMINE:SBA-15			STATISTICS	
	daily		*daily*	*Daily*	*every 5 days*	*every 10 days*	*one-way ANOVA*	*p value*
Brain (g)	0.41 ± 0.03	ip	0.42 ± 0.06	0.41 ± 0.02	0.37 ± 0.08	0.39 ± 0.04	F (4, 40) = 0.712	$p = 0.595$
		oral	0.40 ± 0.05	0.37 ± 0.07	0.36 ± 0.06	*n.d.**	F (3, 39) = 1.326	$p = 0.285$
Lungs (g)	0.17 ± 0.03	ip	0.19 ± 0.04	0.23 ± 0.07	0.21 ± 0.06	0.19 ± 0.04	F (4, 40) = 0.355	$p = 0.836$
		oral	0.15 ± 0.01	0.15 ± 0.02	0.13 ± 0.01	*n.d.**	F (3, 39) = 0.462	$p = 0.711$
Kidneys (g)	0.31 ± 0.03	ip	0.29 ± 0.04	0.30 ± 0.02	0.32 ± 0.03	0.32 ± 0.03	F (4, 40) = 0.961	$p = 0.442$
		oral	0.29 ± 0.03	0.29 ± 0.04	0.28 ± 0.02	*n.d.**	F (3, 39) = 0.563	$p = 0.643$
Liver (g)	1.19 ± 0.16	ip	1.12 ± 0.12	1.14 ± 0.14	1.19 ± 0.18	1.26 ± 0.20	F (4, 40) = 1.696	$p = 0.177$
		oral	1.11 ± 0.08	1.05 ± 0.16	1.12 ± 0.18	*n.d.**	F (3, 39) = 0.713	$p = 0.552$
Femur (cm)	1.59 ± 0.21	ip	1.73 ± 0.05	1.66 ± 0.11	1.68 ± 0.10	*n.d.**	F (4, 40) = 0.710	$p = 0.595$
		oral	1.64 ± 0.09	1.67 ± 0.07	1.61 ± 0.10	*n.d.**	F (3, 39) = 0.915	$p = 0.445$

* non-determined (n.d.).

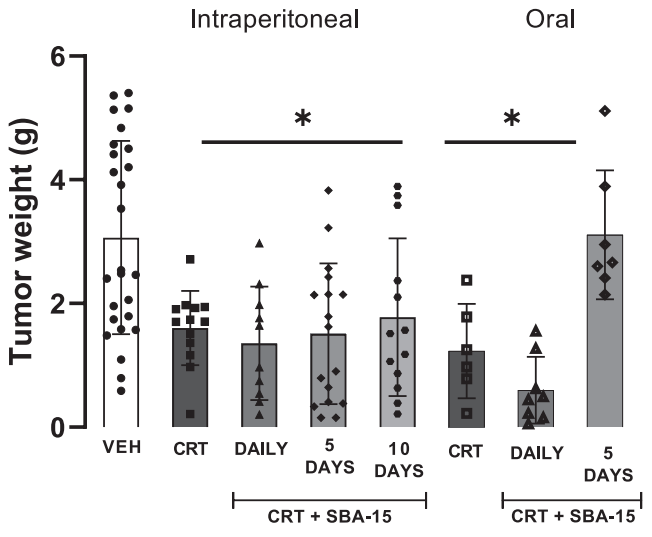

Fig. 5. *In vivo* activity on tumor growth following treatment with crotamine by intraperitoneal administration. Mean weight of tumor tissues (in g ± SD) from the control group, which received the vehicle daily (100 μL/animal; crotamine alone daily (1 μg/animal) ($p < 0.01$); crotamine:SBA-15 (1:1) complex daily ($p < 0.01$), every 5 ($p < 0.01$) or every 10 days ($p = 0.04$). The tumor tissue was removed from all animals at the end of the experimental period of about 21 days. The results correspond to a total of N = 101 animals, *$p \leq 0.05$ for one-way ANOVA test.

schedule demonstrated to be limited. It is also worth emphasizing that every 10-days treatment plan corresponds to only 2 administrations of crotamine (2 μg/animal in 21 days of treatment), which is 90% less than the amount required for daily treatment (21 μg/animal in 21 days of treatment) or 60% less than the 5-days schedule (5 μg/animal in 21 days of treatment). Remarkably the conjugation by adsorption to the SBA-15 nanosilica particles showed similar *in vivo* antitumor effects to those observed for daily treatment with crotamine alone, while decreasing the administration frequency was advantageous only for ip route treatments, it was detrimental for oral treatments with SBA-15 adsorbed crotamine. Interestingly, SBA-15 was used by oral route to improve the efficacy of several compounds (Ambrogi et al., 2012; Scaramuzzi et al., 2016; Sant'Anna et al., 2019; Sant'Anna et al., 2020), but the cationic features of crotamine polypeptide seem to interfere with the slow delivery property of this mesoporous nanoparticle once delivered by gavage into animal gastric compartment, in which the low pH condition may lead to faster release of crotamine, as we have demonstrated here (Fig. 4).

It is also important to mention here that in a previous study, aiming to determine the doses of crotamine needed to affect a shift from parenteral to oral treatment, we have evaluated daily oral crotamine doses of 3, 5 and 10 μg/animal, with significant inhibition of tumor growth with all doses being achieved. However, only the oral administration of crotamine at 10 μg/animal was as effective as the daily intraperitoneal treatment with 1 μg/animal. A higher dispersion and only a trend for a decreased tumor size was noticed for crotamine doses of 3 or 5 μg/animal for daily treatment by oral route (Campeiro et al., 2018), and the present data suggest that the association with SBA-15

may possibly contribute to decrease the amount of crotamine needed for oral treatment (noticed by the smaller dispersion of the data).

Despite the significant decrease in tumor growth shown here, we also observed a higher variation in tumor size in the groups with lower frequency of treatment by ip route, *i.e.* for each 5- or each 10-days schedule, compared with the groups treated daily. Therefore, we believe that there is still room to optimize the treatment protocols with crotamine by evaluating intermediary frequency (as for instance, every 3 days) or alternatively by increasing the doses (>1 μg/animal) for every 5- or 10-days regimen, which we expect to be potentially safer if conjugated with the SBA-15 nanosilica particles, or even by varying the ratio employed for crotamine and SBA-15 association.

This nanostructured mesoporous silica SBA-15, with its unique porous structures and adsorption properties, has also been suggested to improve the immune response (Carvalho et al., 2010; Wang et al., 2012; Liu et al., 2018; Daneluti et al., 2019). This has prompted us to consider if crotamine's improved antitumor effect, given such low doses as those employed here, could have also benefited from activation of the immune system by this silica nanoparticle. This hypothesis may open up new possibilities for preclinical and clinical investigations of the molecular mechanisms underlying the antitumor properties of this polypeptide. New experiments more specifically devoted to this activity are currently being planned in order to explore this highly interesting and important point. Interestingly, the crucial role of the immune system in combatting cancer are widely discussed by many [Ahn et al., 2023; Biri-Kovács et al., 2023; Li et al., 2023]. However, there is still only a single report suggesting that crotamine may stimulate the immune system (Lee et al., 2016). Therefore, further studies may contribute to a better understanding of the molecular mechanisms involved in this polypeptide's inhibition of tumor proliferation including inhibition of other tumor types in addition to exploring the possible contribution of the immune system in reducing tumor bioburden could be of significant value.

5. Conclusions

The adsorption of crotamine in mesoporous SBA-15 nanosilica was demonstrated here by XRD and DLS analysis, in addition to TEM images. This association was demonstrated to improve the pharmacological antitumor effect of crotamine in a murine model for subcutaneous solid tumor, either for intraperitoneal or oral administrations, although the release of crotamine was also demonstrated to be faster under acidic conditions, as those expected to be found in the mice stomach. The use of the mesoporous SBA-15 silica as a carrier for the controlled release of crotamine may represent a feasible approach to decrease the total amount of crotamine needed to control the tumor growth, while also improving its safety by reducing the dosing frequency needed for effective antitumor activity.

Institutional Review Board Statement: The animal study protocol was approved by the Ethic Committee for Animal Use (CEUA) of UNIFESP/EPM (approval No. 6237220116).

Data Availability Statement: The data supporting reported results can be obtained with the corresponding authors with reasonable request.

CRediT authorship contribution statement

William Yoshio Oyadomari: Formal analysis, Investigation, Data curation, Writing – original draft, Writing – review & editing, Funding acquisition. **Gabriel Lessa Anthero:** Investigation, Writing – original draft, Writing – review & editing. **Marcos R. de A. Silva:** Formal analysis, Investigation, Writing – review & editing. **Lucas C. Porta:** Methodology, Formal analysis, Investigation, Writing – review & editing. **Vitor Oliveira:** Methodology, Writing – review & editing, Project administration. **Paul F. Reid:** Writing – original draft, Writing – review & editing. **Osvaldo A. Sant'Anna:** Conceptualization, Writing – review & editing. **Wendel A. Alves:** Formal analysis, Writing – original draft, Writing – review & editing. **João V. Nani:** Methodology, Formal analysis, Investigation, Data curation, Writing – original draft, Writing – review & editing. **Mirian Akemi Furuie Hayashi:** Conceptualization, Methodology, Formal analysis, Investigation, Resources, Writing – original draft, Writing – review & editing, Project administration, Funding acquisition.

Declaration of Competing Interest

The authors declare that they have no known competing financial interests or personal relationships that could have appeared to influence the work reported in this paper.

Data availability

The authors are unable or have chosen not to specify which data has been used.

Acknowledgements

This work was supported by FAPESP (Fundação de Amparo à Pesquisa do Estado de São Paulo) [No. 2022/00527-8; 2020/01107-7; 2019/13112-8; 2019/08287-3; 2017/02413-1; 2014/50891-1 (INCT 2014 - TRANSLATIONAL MEDICINE), 2011/50963-4], FINEP (04.16.0054.02), CAPES and CNPq. MAF Hayashi is also a recipient of a fellowship from CNPq [39337/2016-0]. João V. Nani is recipient of a Fellowship from FAPESP No. 2022/03297-3 and 2019/09207-3).

References

Ahn, R., Cui, Y., White, F.M., 2023. Antigen discovery for the development of cancer immunotherapy. Semin. Immunol. 66, 101733 https://doi.org/10.1016/j.smim.2023.101733.

Ambrogi, V., Perioli, L., Pagano, C., Marmottini, F., Ricci, M., Sagnella, A., Rossi, C., 2012. Use of SBA-15 for furosemide oral delivery enhancement. Eur. J. Pharm. Sci. 46 (1–2), 43–48. https://doi.org/10.1016/j.ejps.2012.02.004.

Biri-Kovács, B., Bánóczi, Z., Tummalapally, A., Szabó, I., 2023. Peptide vaccines in melanoma: chemical approaches towards improved immunotherapeutic efficacy. Pharmaceutics 15 (2), 452. https://doi.org/10.3390/pharmaceutics15020452.

Cai, L., Zhu, P., Huan, F., Wang, J., Zhou, L., Jiang, H., Ji, M., Chen, J., 2021. Toxicity-attenuated mesoporous silica Schiff-base bonded anticancer drug complexes for chemotherapy of drug resistant cancer. Colloids Surf. B Biointerfaces 205, 111839. https://doi.org/10.1016/j.colsurfb.2021.111839.

Campeiro, J.D., Marinovic, M.P., Carapeto, F.C., Dal Mas, C., Monte, G.G., Carvalho Porta, L., Nering, M.B., Oliveira, E.B., Hayashi, M.A.F., 2018. Oral treatment with a rattlesnake native polypeptide crotamine efficiently inhibits the tumor growth with no potential toxicity for the host animal and with suggestive positive effects on animal metabolic profile. Amino Acids 50 (2), 267–278. https://doi.org/10.1007/s00726-017-2513-3.

Carvalho, L.V., Ruiz, R.D.C., Scaramuzzi, K., Marengo, E.B., Matos, J.R., Tambourgi, D. V., et al., 2010. Immunological parameters related to the adjuvant effect of the ordered mesoporous silica SBA-15. Vaccine 28, 7829–7836. https://doi.org/10.1016/j.vaccine.2010.09.087.

Dadej, A., Woźniak-Braszak, A., Bilski, P., Piotrowska-Kempisty, H., Józkowiak, M., Stawny, M., Dadej, D., Mrotek, M., Jelińska, A., 2022a. APTES-modified SBA-15 as a non-toxic carrier for phenylbutazone. Materials (Basel) 15 (3), 946. https://doi.org/10.3390/ma15030946.

Dadej, A., Woźniak-Braszak, A., Bilski, P., Piotrowska-Kempisty, H., Józkowiak, M., Pawełczyk, A., Dadej, D., Łażewska, D., Jelińska, A., 2022b. Improved solubility of lornoxicam by inclusion into SBA-15: comparison of loading methods. Eur. J. Pharm. Sci. 171, 106133 https://doi.org/10.1016/j.ejps.2022.106133.

Daneluti, A.L.M., Neto, F.M., Ruscinc, N., Lopes, I., Robles Velasco, M.V., Matos, D.R., J.,, et al., 2019. Using ordered mesoporous silica SBA-15 to limit cutaneous penetration and transdermal permeation of organic UV filters. Int. J. Pharm. 570, 118633 https://doi.org/10.1016/j.ijpharm.2019.118633.

de Carvalho Porta, L., Fadel, V., D'Arc Campeiro, J., Oliveira, E.B., Godinho, R.O., Hayashi, M.A.F., 2020. Biophysical and pharmacological characterization of a full-length synthetic analog of the antitumor polypeptide crotamine. J. Mol. Med. (Berl) 98 (11), 1561–1571. https://doi.org/10.1007/s00109-020-01975-y.

Dong, M., Lin, J., Lim, W., Jin, W., Lee, H.J., 2018. Role of brown adipose tissue in metabolic syndrome, aging, and cancer cachexia. Front. Med. 12, 130–138.

Fantini, M., Matos, J., Cides, L.C., Mercuri, L., Chiereci, G.O., Celer, E.B., Jaroniec, M., 2004. Ordered mesoporous silica: microwave synthesis. Mater. Sci. Eng. B 112, 106–110. https://doi.org/10.1016/j.mseb.2004.05.013.

García-Muñoz, R.A., Morales, V., Linares, M., González, P.E., Sanz, R., Serrano, D.P., 2014. Influence of the structural and textural properties of ordered mesoporous materials and hierarchical zeolitic supports on the controlled release of

methylprednisolone hemisuccinate. J. Mater. Chem. B 2 (45), 7996–8004. https://doi.org/10.1039/c4tb00089g.
Hayashi, M.A.F., Campeiro, J.D., Yonamine, C.M., 2022. Revisiting the potential of South American rattlesnake *Crotalus durissus terrificus* toxins as therapeutic, theranostic and/or biotechnological agents. Toxicon 206, 1–13. https://doi.org/10.1016/j.toxicon.2021.12.005.
Hayashi, M.A., Nascimento, F.D., Kerkis, A., Oliveira, V., Oliveira, E.B., Pereira, A., Rádis-Baptista, G., Nader, H.B., Yamane, T., Kerkis, I., Tersariol, I.L., 2008. Cytotoxic effects of crotamine are mediated through lysosomal membrane permeabilization. Toxicon 52 (3), 508–517. https://doi.org/10.1016/j.toxicon.2008.06.029.
Hayashi, M.A., Ducancel, F., Konno, K., 2012. Natural peptides with potential applications in drug development, diagnosis, and/or biotechnology. Int. J. Pept. 2012, 757838 https://doi.org/10.1155/2012/757838.
Lee, K.J., Kim, Y.K., Krupa, M., Nguyen, A.N., Do, B.H., Chung, B., Vu, T.T., Kim, S.C., Choe, H., 2016. Crotamine stimulates phagocytic activity by inducing nitric oxide and TNF-α via p38 and NFκ-B signaling in RAW 264.7 macrophages. BMB Rep. 49 (3), 185–190. https://doi.org/10.5483/bmbrep.2016.49.3.271.
Li, D., Li, W., Zheng, P., Yang, Y., Liu, Q., Hu, Y., He, J., Long, Q., Ma, Y., 2023. A "trained immunity" inducer-adjuvanted nanovaccine reverses the growth of established tumors in mice. J. Nanobiotechnology 21 (1), 74. https://doi.org/10.1186/s12951-023-01832-3.
Lima, S.C., Porta, L.C., Lima, Á.D.C., Campeiro, J.D., Meurer, Y., Teixeira, N.B., Duarte, T., Oliveira, E.B., Picolo, G., Godinho, R.O., Silva, R.H., Hayashi, M.A.F., 2018. Pharmacological characterization of crotamine effects on mice hind limb paralysis employing both *ex vivo* and *in vivo* assays: insights into the involvement of voltage-gated ion channels in the crotamine action on skeletal muscles. PLoS Negl. Trop. Dis. 12 (8), e0006700.
Liu, X., Gu, Y.-L., Zhang, B.-B., Dong, Q.-M., Li, Y.-L., Wang, H.-M., 2018. The construction of sustained-release systems of tanshinone IIA and sodium tanshinone IIA sulfonate by SBA-15 mesoporous material. J. Nanosci. Nanotechnol. 19, 956–962.
Lopez, T., Ortiz, E., Alexander-Katz, R., Basaldella, E., Bokhimi, X., 2009. Cortisol controlled release by mesoporous silica. Nanomedicine 5 (2), 170–177. https://doi.org/10.1016/j.nano.2008.08.002.
Lu, J., Liong, M., 2011. Biocompatibility, biodistribution, and drug delivery efficiency of mesoporous silica nanoparticles for cancer therapy in animals. Small 6, 1794–1805. https://doi.org/10.1002/smll.201000538.Biocompatibility.
Marinovic, M.P., Campeiro, J.D., Lima, C., Rocha, A.L., Nering, M.B., Oliveira, E.B., Mori, M.A., Hayashi, M.A.F., 2018. Crotamine induces browning of adipose tissue and increases energy expenditure in mice. Sci. Rep. 8 (1), 5057. https://doi.org/10.1038/s41598-018-22988-1.
Matos, J.R., Mercuri, L.P., Kruk, M., Jaroniec, M., 2001. Toward the synthesis of extra-large-pore MCM-41 analogues. Chem. Mater. 13, 1726–1731.
Nascimento, F.D., Hayashi, M.A., Kerkis, A., Oliveira, V., Oliveira, E.B., Rádis-Baptista, G., Nader, H.B., Yamane, T., Tersariol, I.L., Kerkis, I., 2007. Crotamine mediates gene delivery into cells through the binding to heparan sulfate proteoglycans. J. Biol. Chem. 282 (29), 21349–21360. https://doi.org/10.1074/jbc.M604876200.
Nascimento, F.D., Sancey, L., Pereira, A., Rome, C., Oliveira, V., Oliveira, E.B., Nader, H. B., Yamane, T., Kerkis, I., Tersariol, I.L., Coll, J.L., Hayashi, M.A., 2012. The natural cell-penetrating peptide crotamine targets tumor tissue *in vivo* and triggers a lethal calcium-dependent pathway in cultured cells. Mol. Pharm. 9 (2), 211–221. https://doi.org/10.1021/mp2000605.
Pereira, A., Kerkis, A., Hayashi, M.A., Pereira, A.S., Silva, F.S., Oliveira, E.B., Prieto da Silva, A.R., Yamane, T., Rádis-Baptista, G., Kerkis, I., 2011. Crotamine toxicity and efficacy in mouse models of melanoma. Expert Opin. Invest. Drugs 20 (9), 1189–1200. https://doi.org/10.1517/13543784.2011.602064.
Porta, L.C., Campeiro, J.D., Hayashi, M.A.F., 2022. A native CPP from rattlesnake with therapeutic and theranostic properties. Methods Mol. Biol. 2383, 91–104. https://doi.org/10.1007/978-1-0716-1752-6_6.
Predarska, I., Saoud, M., Drača, D., Morgan, I., Komazec, T., Eichhorn, T., Mihajlović, E., Dunđerović, D., Mijatović, S., Maksimović-Ivanić, D., Hey-Hawkins, E., Kaluđerović, G.N., 2022. Mesoporous silica nanoparticles enhance the anticancer efficacy of platinum(IV)-phenolate conjugates in breast cancer cell lines. Nanomaterials (Basel) 12 (21), 3767. https://doi.org/10.3390/nano12213767.
Rehman, F., Rahim, A., Airoldi, C., Volpe, P.L.O., 2016. Preparation and characterization of glycidyl methacrylate organo bridges grafted mesoporous silica SBA-15 as ibuprofen and mesalamine carrier for controlled release. Mater. Sci. Eng. C Mater. Biol. Appl. 59, 970–979. https://doi.org/10.1016/j.msec.2015.11.005.
Rehman, F., Khan, A.J., Sama, Z.U., Alobaid, H.M., Gilani, M.A., Safi, S.Z., Muhammad, N., Rahim, A., Ali, A., Guo, J., Arshad, M., Emran, T.B., 2023. Surface engineered mesoporous silica carriers for the controlled delivery of anticancer drug 5-fluorouracil: computational approach for the drug-carrier interactions using density functional theory. Front. Pharmacol. 14, 1146562. https://doi.org/10.3389/fphar.2023.1146562.
Sant'Anna, M.B., Lopes, F.S.R., Kimura, L.F., Giardini, A.C., Sant'Anna, O.A., Picolo, G., 2019. Crotoxin conjugated to SBA-15 nanostructured mesoporous silica induces long-last analgesic effect in the neuropathic pain model in mice. Toxins (Basel) 11 (12), 679. https://doi.org/10.3390/toxins11120679.
Sant'Anna, M.B., Giardini, A.C., Ribeiro, M.A.C., Lopes, F.S.R., Teixeira, N.B., Kimura, L. F., Bufalo, M.C., Ribeiro, O.G., Borrego, A., Cabrera, W.H.K., Ferreira, J.C.B., Zambelli, V.O., Sant'Anna, O.A., Picolo, G., 2020. The Crotoxin:SBA-15 complex down-regulates the incidence and intensity of experimental autoimmune encephalomyelitis through peripheral and central actions. Front. Immunol. 11, 591563 https://doi.org/10.3389/fimmu.2020.591563.
Scaramuzzi, K., Tanaka, G.D., Neto, F.M., Garcia, P.R., Gabrili, J.J., Oliveira, D.C., Tambourgi, D.V., Mussalem, J.S., Paixão-Cavalcante, D., D'Azeredo Orlando, M.T., Botosso, V.F., Oliveira, C.L., Fantini, M.C., Sant'Anna, O.A., 2016. Nanostructured SBA-15 silica: an effective protective vehicle to oral hepatitis B vaccine immunization. Nanomedicine 12 (8), 2241–2250. https://doi.org/10.1016/j.nano.2016.06.003.
Schlossbauer, A., Dohmen, C., Schaffert, D., Wagner, E., Bein, T., 2011. pH-responsive release of acetal-linked melittin from SBA-15 mesoporous silica. Angew. Chem. Int. Ed. Engl. 50 (30), 6828–6830. https://doi.org/10.1002/anie.201005120.
Tan, H., Yang, S., Dai, P., Li, W., Yue, B., 2015. Preparation and physical characterization of calcium sulfate cement/silica-based mesoporous material composites for controlled release of BMP-2. Int. J. Nanomed. 10, 4341–4350. https://doi.org/10.2147/IJN.S85763.
Vieira, C.O., Grice, J.E., Roberts, M.S., Haridass, I.N., Duque, M.D., Lopes, P.S., et al., 2019. ZnO:SBA-15 nanocomposites for potential use in sunscreen: preparation, properties, human skin penetration and toxicity. Skin Pharmacol. Physiol. 32, 32–42. https://doi.org/10.1159/000491758.
Wang, T., Jiang, H., Zhao, Q., Wang, S., Zou, M., Cheng, G., 2012. Enhanced mucosal and systemic immune responses obtained by porous silica nanoparticles used as an oral vaccine adjuvant: effect of silica architecture on immunological properties. Int. J. Pharm. 436, 351–358. https://doi.org/10.1016/j.ijpharm.2012.06.028.
Yamane, E.S., Bizerra, F.C., Oliveira, E.B., Moreira, J.T., Rajabi, M., Nunes, G.L., de Souza, A.O., da Silva, I.D., Yamane, T., Karpel, R.L., Silva Jr., P.I., Hayashi, M.A., 2013. Unraveling the antifungal activity of a South American rattlesnake toxin crotamine. Biochimie 95 (2), 231–240. https://doi.org/10.1016/j.biochi.2012.09.019.
Yoo, J.-W., Irvine, D.J., Discher, D.E., Mitragotri, S., 2011. Bio-inspired, bioengineered and biomimetic drug delivery carriers. Nat. Rev. Drug Discov. 10, 521–535. https://doi.org/10.1038/nrd3499.
Zholkovskij, E.K., Masliyah, J.H., Shilov, V.N., Bhattacharjee, S., 2007. Electrokinetic phenomena in concentrated disperse systems: general problem formulation and spherical cell approach. Adv. Colloid Interface Sci. 134–135, 279–321. https://doi.org/10.1016/j.cis.2007.04.025.